Challenging Glass 5 – Conference on Architectural and Structural Applications of Glass
Belis, Bos & Louter (Eds.), Ghent University, June 2016.

ISBN 978-90-825-2680-6

Structural Glazing: Design under High Windload

P. Descamps[a], J. Kimberlain[b], J. Bautista[c] & P. Vandereecken[a]
[a] *Dow Corning Corporation, Belgium, Patrick.vandereecken@dowcorning.com*
[b] *Dow Corning Corporation, Midland, United States*
[c] *Dow Corning Corporation, Singapore*

Bonding of glass onto aluminum frames, known as "Structural Silicone Glazing", has been applied for more than 40 years in glass curtain wall facades. Silicone sealants are being used in this application because of their outstanding resistance to weathering (UV, temperature, moisture, ozone), They also provide resistance to water egress and thermal insulation. Their role, structurally, is to resist to windloads and to compensate for differential thermal expansion of glass and aluminum frame. For windload resistance, silicone bite is calculated using a simplified equation which assumes a uniform stress distribution along the sealant bite. Finite Element Analysis (FEA) was used in this study calculate the stress distribution in the sealant as a function of sealant bite and thickness and show the importance of the sealant geometry (bite and thickness) on the local stress distribution. The study shows that for glass deflections in the 1% region (L/d=100), large sealant joints and/or high modulus sealants lead to higher local stresses.

Keywords: Structural Glazing, silicone sealant, Finite Element Analysis

1. Introduction

Structural silicone glazing has a long history of proven performance on building facades. The engineering practice of glass bonding dates back to the mid 1960's evolving into being the sole mean of retention for glass on the face of building in the early 1970's, with the original project still in service. Evolution of the practice has continued with improvements such as sealant chemistry to facilitate rapid manufacturing with the commercialization of two part sealants in the early 1980's. New trends including the use of large glass sizes, sophisticated engineering analysis using finite element analysis and stronger engineering performance such as high windloads have recently challenged the conventional methods of design to continue this evolution. Answering these challenges should be expected to enhance long term performance in challenging environments for a proven technology. The paper uses finite element analysis to better understand the impact of design geometry, windloads and sealant performance to understand the challenges in this continued evolution.

2. New trends

Use of large glasses in places under high windloads is one of the new trends in commercial buildings. Today it is not uncommon to design systems assuming a windload above 5kPa. Current standards for structural glazing (ASTM C1401, ETAG002, GB16776) consider trapezoidal glass deformation with homogeneous stress distribution within the sealant bite. This means that the sealant bite is proportional to the glass size (small dimension) and to the windload and inversely proportional to the sealant design strength as shown in eqn 1 where b is the sealant structural bite, a is the shortest lite dimension, WL is windload and σdes is the allowable design stress.

$$b = 0.5 * a * WL / \sigma_{des} \qquad (1)$$

Using sealants with a design stress of 140 kPa, bites become rapidly unacceptable (>30mm) for large glasses and projects under high windloads.Those large bites lead to the need to increase aluminium profile widths, thereby increasing the costs and decreasing building energy performance. Increasing the sealant design strength would be an option to decrease the sealant bite but increasing the sealant modulus leads to increased stresses under daily thermal deformation (figure 1).

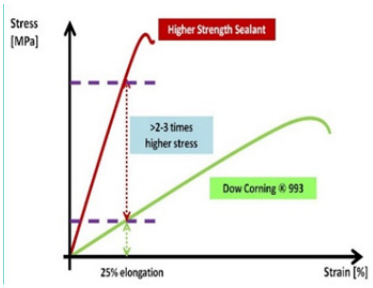

Fig. 1 Stress in function of elongation for sealant of different modulus (stiffness).

In projects with large glasses and high windloads, glass deflection is usually above 1% (L/d > 60) as maintaining the glass deflection below 1% would lead to the increase of glass thickness, thereby again increasing project costs. However, under high glass deflection, the assumption of homogeneous stress distribution along the sealant bite is not valid anymore. This was already briefly mentioned in an annex of an ETAG002 report (2006). In this report, an additional term accounts for effect of glass deflection on the sealant stress (eqn 2). This additional term is a function of sealant rigidity (ER), glass deflection (α) and sealant thickness (e) and also sealant bite.

$$\sigma = 0.5 * a * WL / b + ((b * \alpha * E_R)/ (2*e)) \qquad (2)$$

This equation already indicated that increasing the sealant bite and/or sealant stiffness can have a negative effect on the sealant stress. Finite Element Analysis (FEA) softwares are nowadays available and should allow us to have a better insight into the stress distribution of a sealant bead. Next paragraph discusses an FEA sealant stress distribution study for cases where glass deflection is between 1 and 2%. The study shows the effect of increasing sealant bite and sealant modulus on stress distribution.

3. FEA simulations

3.1 Selection and validation of an hyper-elastic material model

The first step in structural mechanics FEA modelling is to select a model that describes the behavior of material in a satisfactory way. If silicone sealants show a linear behavior for small elongations, behavior deviates from linearity when elongation increases and in this region, a linear model is no more satisfactory. In the process of identifying a nonlinear model for material description, a good practice is to start with the simpler non-linear model i.e. the Neo-Hookean model with ν (Poisson coefficient) being set close to 0.5. Experimental data from dog bone test samples are used to obtain a pure uniaxial stress i.e. the principal stress diagonal matrix having a sole non null element. In nearly uncompressible Neo-Hookean model, the strain energy is written (equation 3) in terms of the elastic volume ratio Je and the first invariant of the elastic right Cauchy-Green deformation tensor I1 (Feynman 1961-1963):

$$W = \frac{1}{2}\,\mu\,(I1 - 3) + \frac{1}{2}\,k\,(Je - 1)^2 \qquad (3)$$

Where parameter μ and k are the shear modulus and the initial bulk modulus of the material.

k and μ are the free parameters for fitting the engineering strain/stress curve calculated from a 3D simulation of a dog bone test piece to the Strain/stress curve measured experimentally; via curve fitting, we obtain μ = 0.77e6 Pa and k=38.3e6 Pa for DC 993.

To validate material model, we simulate two H-pieces of different geometries, calculating the elongation in function of tension force. Test pieces are prepared and tested using a Zwick tensiometer, recording the experimental Stress/Strain curve. Because the incompressibility of adhesion plane explained in paragraph below, both the model and the experiment show an apparent rigidity modulus greater than the value measured on the dog bone test piece. A good agreement between the model and experiment is observed for the two different test piece geometries (figure 2) showing that a Neo-Hookean model provides an acceptable description of silicone sealant behavior.

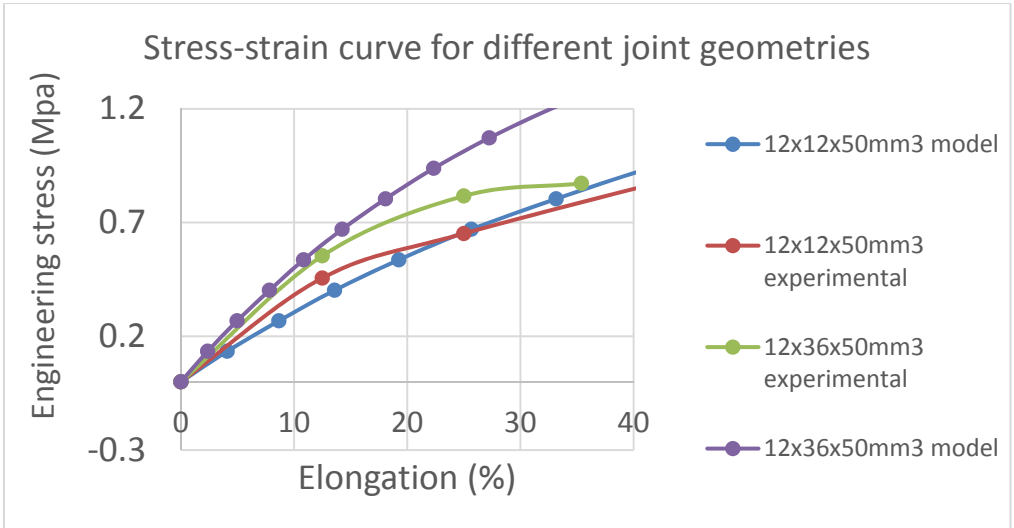

Fig. 2 Comparison between the stress- strain curves measured on H-pieces of two different geometries and the prediction of a 3D model of these H-pieces.

3.2 Mesh selection

One critical aspect in FEA resolution of physic equations (structural mechanical, Navier-Stokes, thermal transfer,...) is the proper mesh setting, an exercise strongly depending on the physics of the problem to be solved. An important criteria in mesh selection is to guarantee that the size of the mesh element is small compared to the gradient of the variable being calculated in a way to guarantee that equation discretization provides an adequate picture of the physic under study.

This requirement is critical when calculating stress build-up within an adhesive bound to a substrate. To illustrate this point, we assume a block of linear elastic material with a force being applied to two opposite faces of the block. In (Feynman 1961-1963), the rigidity modulus of this system is calculated assuming no change in block cross-section. It is demonstrated that equivalent rigidity modulus of the block is simply (equation 4):

$$E_{eq} = E_{Young} \frac{(1-\nu)}{(1+\nu)(1-2\nu)} \qquad (4)$$

Where E_{Young} is material elastic modulus and ν is the Poisson ratio.

From equation 4, we observe that a purely uncompressible material characterized by ν=0.5 has a rigidity modulus equal to infinity. For nearly uncompressible material of Poisson ratio equal to 0.49 or 0.48 respectively, the rigidity modulus is respectively 17 and 9 times larger than material elastic modulus.

Of course, in real joint geometries, this theoretical case of zero x-section reduction under tension assumed in [3] is only approached in an infinitively thin layer close to the plane of adhesion; we expect rigidity modulus to decrease as material x-section "is allowed" to reduce when moving away from the plane of adhesion. This simplified model puts in evidence the existence of large stress gradients close to adhesion plane therefore a special care must be taken in the way the mesh is defined in the vicinity of the substrate.

To illustrate importance of adequate mesh selection at the interface substrate/sealant, the maximum value of the first principal stress is calculated for the geometry represented in figure 3b (25mm joint bite, 6mm joint thickness) using different mesh densities. We observe that increasing mesh density in the vicinity of the adhesion plane leads to an increase of the maximum value of the first principal stress. Above a certain limit, we obtain a stable, mesh insensitive solution.

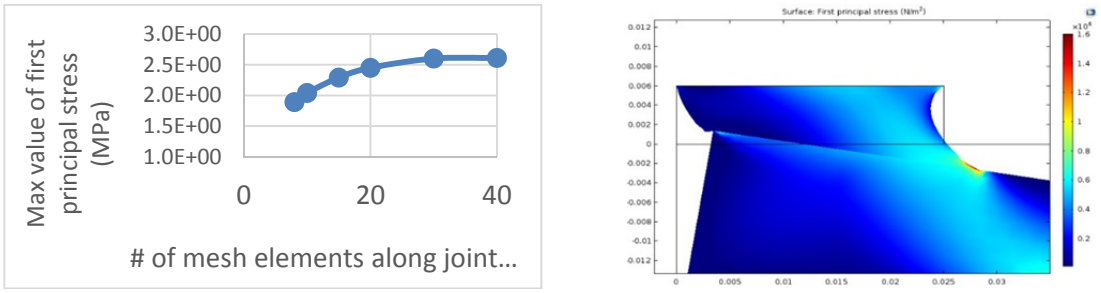

Fig. 3 a) maximum local stress in function of mesh density; b) example of first principal stress spatial distribution.

*3.3. 2D simulation of frame/*joint/glass pane *assembly*

a) Effect of sealant bite on local stress build-up

We simulated in 2D a system made of a 1.9m wide glass pane glued at each side to an infinitely rigid frame using a silicone joint. The thickness of the glass pane is adjusted to obtain a maximum deflection at glass center of respectively 1% and 2% for a wind load of 4920Pa. Calculations are carried-out for 3 joint thicknesses (6, 7.5 and 9mm); for each joint thickness, joint bite is varied between 15 and 40mm. For each joint configuration, the maximum value of the first principal stress is plotted. We also plot on the same graph the stress value calculated if assuming a homogeneous stress distribution in the joint. The results are given on figure 4.

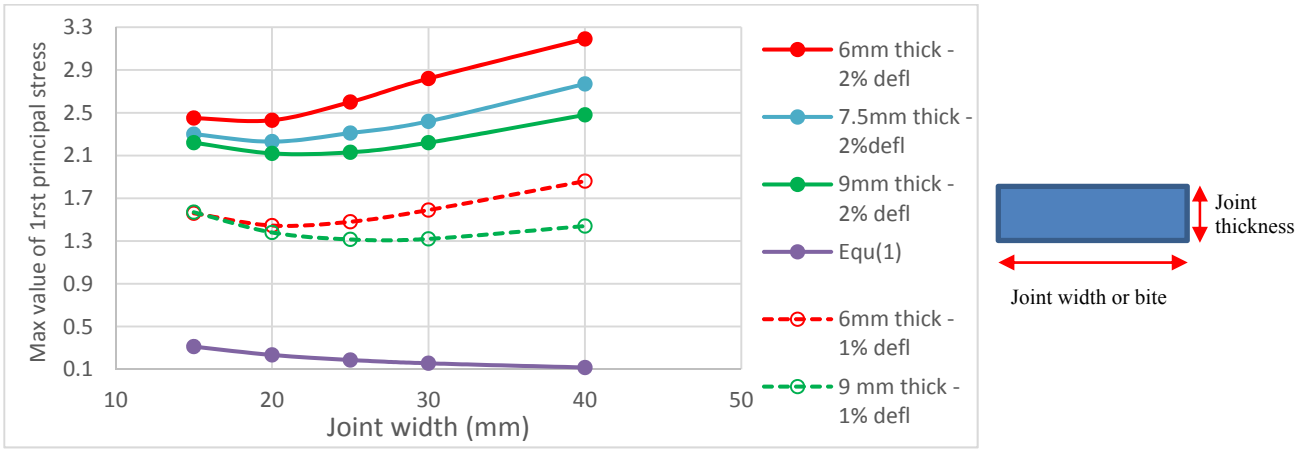

Fig. 4 Maximum value of first principal stress in function of joint bite, joint thickness and glass deflection

As expected, the stress calculated using the assumptions made in equation (1) shows a continuous decrease when increasing joint bite because the stress is assumed homogenously distributed and decreases with the sealant bite. If we consider glass deformation, we observe, using FEA, a decrease of the maximum local stress when increasing joint bite up to 20mm. But, for a bite around 25mm, we observe a saddle point where the trend reverses and maximum local stress starts to increase with joint bite. It is interesting to observe that when increasing joint bite, a fraction of the joint works in compression and does not contribute in sustaining the wind load ~ orthogonal to the glass pane (figure 5).

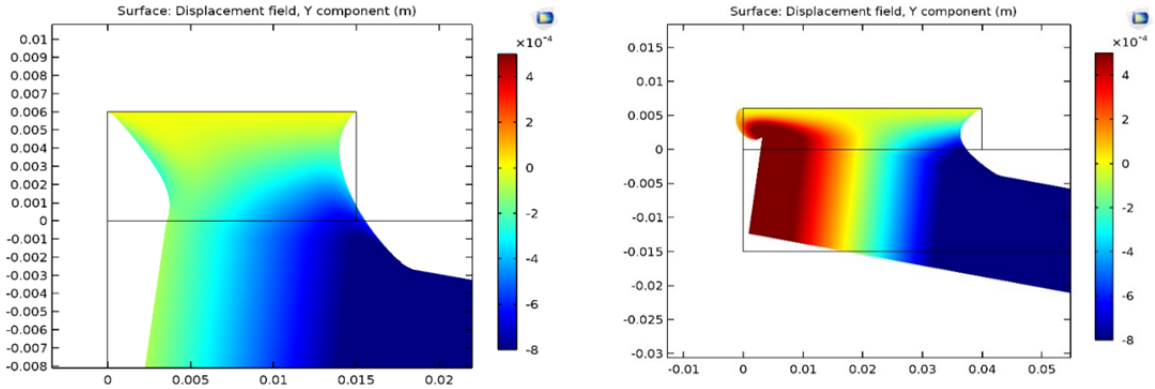

Fig. 5 joint displacement along Y axis, zero displacement corresponding to frame surface – a) for a joint bite of 15mm, displacement is everywhere negative meaning all joint works in traction b) case of a 40mm joint bite, the outer part of the joint (red color) works in compression.

b) Effect of sealant bite on glass deflection

As joint stiffness depends on geometry (stiffness increases with the ratio joint area/joint thickness), there may exist joint designs that influence glass pane deflection compared to the value calculated assuming a simply supported glass pane (i.e. the distance between the fixation points freely decrease as glass pane bends). Because of the presence of silicone joint, lateral displacement of glass sides is not free. To understand the magnitude of this effect, the evolution of maximum deflection at glass center is calculated in function of joint bite for 2 joint thicknesses (figure 6). To illustrate this effect, we calculate the deflection for a rigid joint (joint of 6mm thickness) but assuming a free horizontal translation of the bottom side of the joint (displacement being only constrained perpendicular to joint bite).

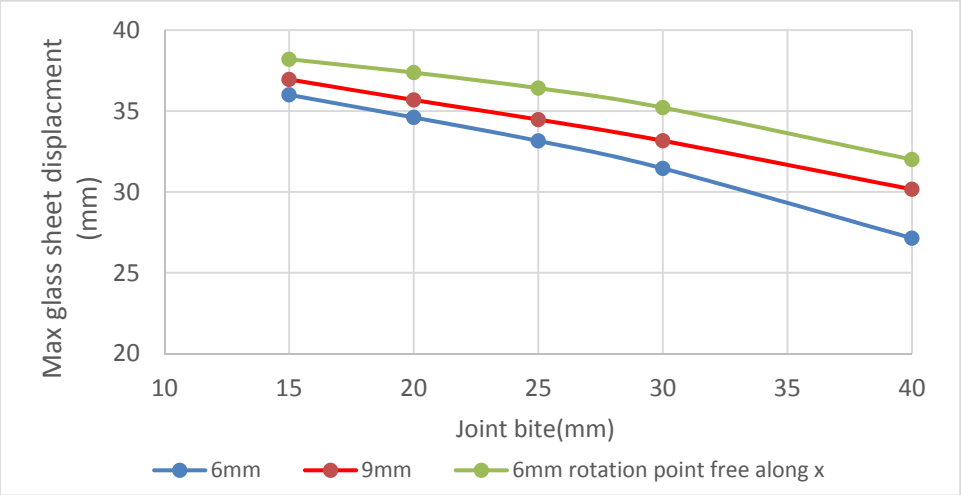

Fig. 6 maximum deflection of glass at its center in function of joint bite, for joint thicknesses of 6 and 9mm.

Figure 6 shows that joints with large joint bite to thickness ratio (stiff joints) lead to restricted glass deflection compared to the simply supported glass pane because the distance between fixing points cannot freely reduce with bending. A fraction of wind load is then transferred as a shear stress in the structural joint. This effect is rather significant and further impacts inhomogeneity of stress distribution in the joint and contributes to local stress increase with joint bite.

c) Effect of sealant elastic modulus on local stress build-up

2D simulation of the frame system is replicated assuming one sealant thickness equal to 6mm but considering three sealants of different elastic modulus. Effect of sealant bite on stress build-up is calculated varying bites between 15 and 40mm (figure 7).

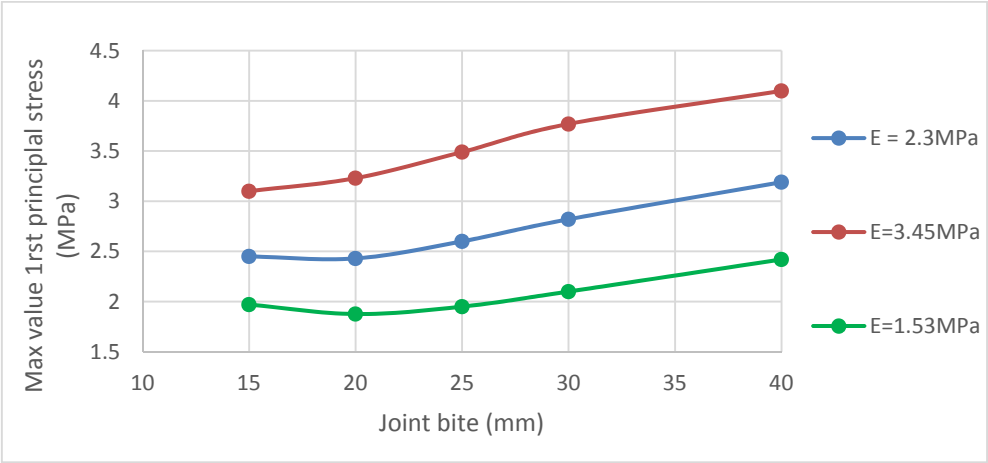

Fig. 7 Evolution of the maximum value of first principal stress in function of joint bite and sealant modulus, for a joint thickness of 6mm. Calculation was carried-out with different values of μ and k corresponding to a material half stiff or two times more stiff compared to standard DC993 material.

Using a lower modulus sealant, local stress is decreased for all joint configurations. The joint thickness corresponding to the minimum is also displaced. For sealant of higher elastic modulus equal to 3.45MPa, the minimum disappears and the local stress increases in a monotone way with joint bite. This result is intuitive because a low modulus sealant shows a larger total joint elongation (large $\Delta e0$) limiting joint compression. On the contrary, a more rigid sealant shows already compression for a relatively small joint bite of 15mm. This calculation demonstrates that using a very rigid material is not suitable when significant glass deformation are considered. From two materials showing the same tensile strength at break measured on test piece, the less rigid material should be preferred. Of course, movement of glass pane with respect to the frame must also be minimized to prevent the glass pane to slide out of the setting block sustaining the dead load. Therefore selection of material rigidity will necessarily be the result of a tradeoff.

3.4 Modelling a 3D geometry

The 2D model has been extended to 3D, incorporating the learning acquired from the 2D simulation effort. The glass pane has 1.9 x 1.4 m2. Glass thickness is 8 mm and glass deflection at center is 20.8 mm (1.5%) for a wind load equal to 5000Pa. Using symmetry, a quarter of the glass pane is modelled. Figures 8 represents the first principal stress calculated for a 20mm joint bite. The stress is calculated in a plane located close to interface between the joint and the supporting frame.

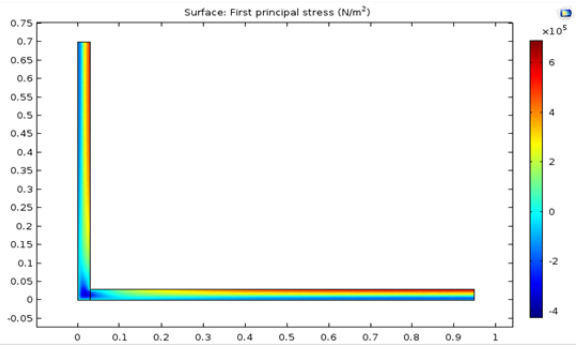

Fig. 8 first principal stress distribution close to the adhesion plane, calculated for a joint bite of 20mm and a joint thickness of 6mm.

As expected, we observe that the stress is maximum in the middle of the frame profile; in the corner, the first principal stress has a negative value, which indicates a local compression of the joint. Changing the joint bite from 15mm to 40mm, we obtain results that are very consistent with 2D simulation, with the existence of a saddle point after which the maximum local stress increases with joint bite. As for the 2D simulation, increasing the joint bite is also characterized by a displacement of the point at which compression takes place in the joint (figure 9).

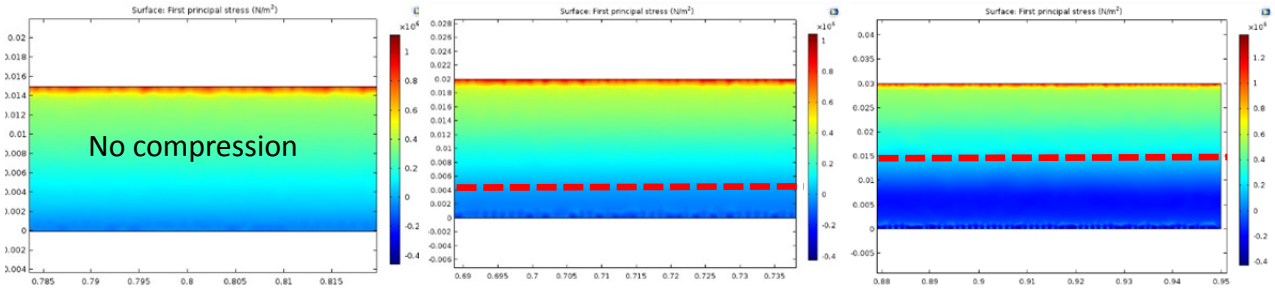

Fig. 9 Distribution of first principal stress close to the interface between the sealant joint and the glass pane. Joint bite is respectively 15, 20 and 30mm. The red dotted line represents the transition from traction to joint compression.

4. Stress distribution within a SSG joint of a facade system and in an H-piece test sample

In above paragraphs, stress distribution is calculated for different joints configurations using the first principal stress. As a second step, we want to understand if the maximum principal stress is the quantity that best describes material damage associated to joint deformation. To answer this critical but very complex question, we must link back to the fundamentals of failure theory. In literature, many different models exists to predict material failure but unfortunately, there is no unique model being successful for predicting failure in all types of materials. For this reason, different failure models were developed which showed some success in predicting failure for a specific family of materials (metals, concrete…).

For example, rupture of a material can be seen as the result of an alteration of the cohesive forces between molecules because of the increased distance between them. From this assumption, it was suggested to use the maximum deformation per unit length criteria, two states of stress being equally dangerous if having the same maximum deformation. Permanent deformation in material like metal often occurs as a result of one plane sliding with respect to another, suggesting that two limit states are equally dangerous if their maximum tangential stress are equal. For ductile materials, it is proposed to use potential energy of deformation but neglecting the contribution associated to volume variation and only keeping potential energy contribution associated to variation of shape, two states being equally dangerous if having the same energy of variation of shape. This assumption leads to the well-known Von Mises stress.

To understand which failure model best describes silicone material, H shape test pieces of different geometries were tested and experimental results confronted to the predictions of different failure models. One very interesting observation coming out H-piece testing is the difference in failure mode depending on test piece geometry: for a 12x12x50mm3 H-piece (12mm thick joint), we observe failure taking place in the bulk of the joint i.e. in the middle

of joint thickness. For a 6x36x50mm3 geometry (6mm thick joint), failure is initiated at the sealant-substrate interface, along the perimeter of the adhesion plane. Rupture then propagates to the center of the joint and when the surface of adhesion plane reaches around 18*30mm2, the zone of rupture is displaced to the bulk of the remaining joint (we can see it as a transition from a boundary failure to a cohesive failure). We used this observation in the process of failure model evaluation, computing the spatial distribution of 1) the maximum principal stress, 2) the maximum principal strain, 3) the maximum shear and 4) the Von Mises Stress to determine which one of these models best explains experimental observations. The goal of this exercise is not to predict failure which is at the stage of this research too ambitious but to provide guidelines about failure model being closer to sealant behavior.

The distribution of maximum principal stress, max principal strain, maximum shear stress and Von Mises stress are calculated:

- In a vertical plane which cuts the test piece in the middle of its long dimension.

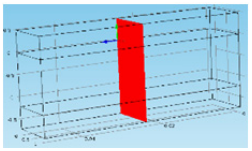

- In 2 horizontal planes (planes parallel to the substrate), one located in the middle of the joint and the second close to the substrate.

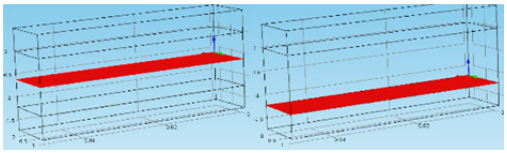

As the material deforms more freely moving away from the substrate, we observe in the horizontal plane located in the middle of the joint that principal component σ1 >> σ2 or σ3; close to the interface, σ2 and σ3 are no more small compared to σ1. As a result, both maximum principal strain, maximum shear and Von Mises stress lead to very similar conclusions. For this reason, we made the choice for purpose of clarity to only show the comparison between the first principal stress and Von Mises stress in the below analysis.

12x12x50mm3 joint

Looking at stress distribution in the vertical plane (figure 10), Von Mises Stress in the joint near the substrate decreases very rapidly when moving from the perimeter to the center of the joint to reach a value below 0.5 MPa (zone in blue color). Except for small regions located in the 4 corners, Von Mises stress is significantly lower at the interface than in the bulk of the joint. Looking at the maximum principal stress value, this effect is less marked and distribution more homogeneous along the interface.

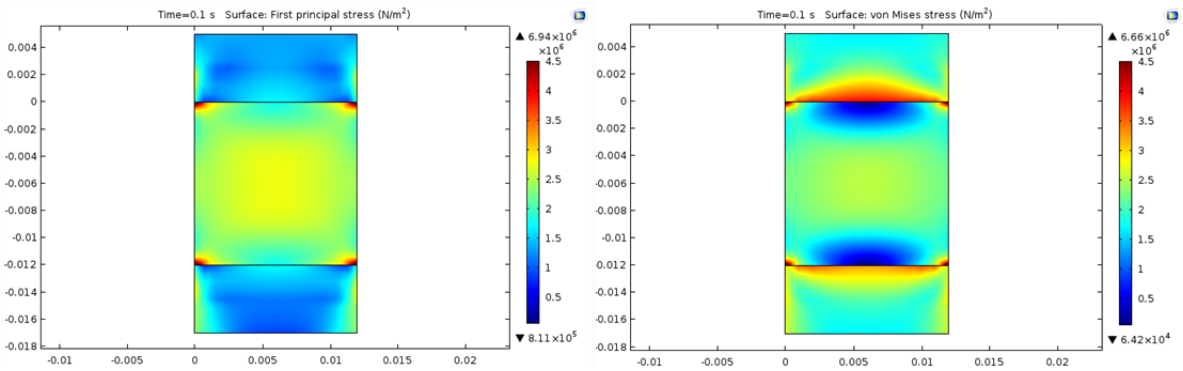

Fig. 10 Spatial distribution of first principal stress (left) and Von Mises stress (right) for a 12x12x50mm3 test piece geometry

Von Mises stress in the horizontal plane close to the substrate shows a more inhomogeneous spatial distribution than the first principal stress, with a very low stress value observed in the center of the plane (figure 11).

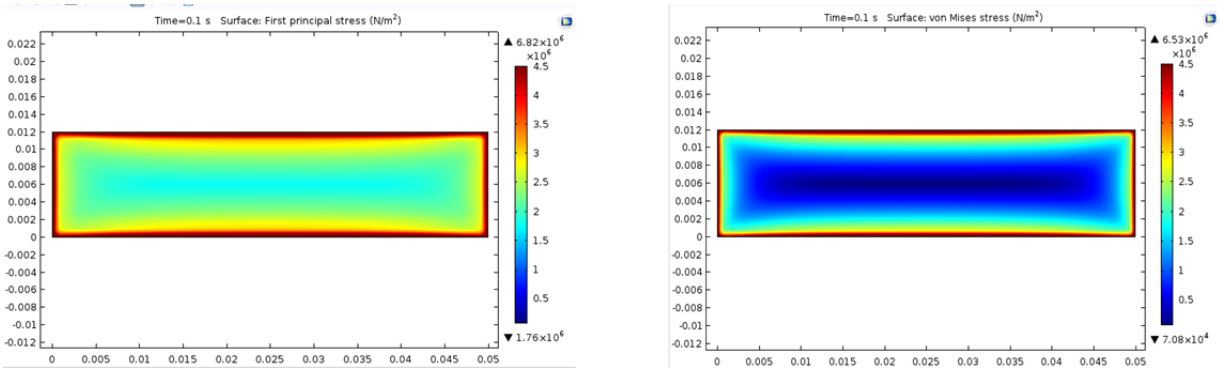

Fig. 11 Spatial distribution of first principal stress (left) and Von Mises stress (right) for the 12x12x50 test piece geometry – Horizontal plane close to the substrate.

In the horizontal plane located in the middle of the joint, the stress distribution is rather homogenous for both first principal stress and Von Mises Stress, a larger value of Von Mises Stress being observed (figure 12). The ratio between maximum stress at the interface and maximum stress is the bulk of the joint is respectively 2.6 for first principal stress and 2.3 for Von Mises stress.

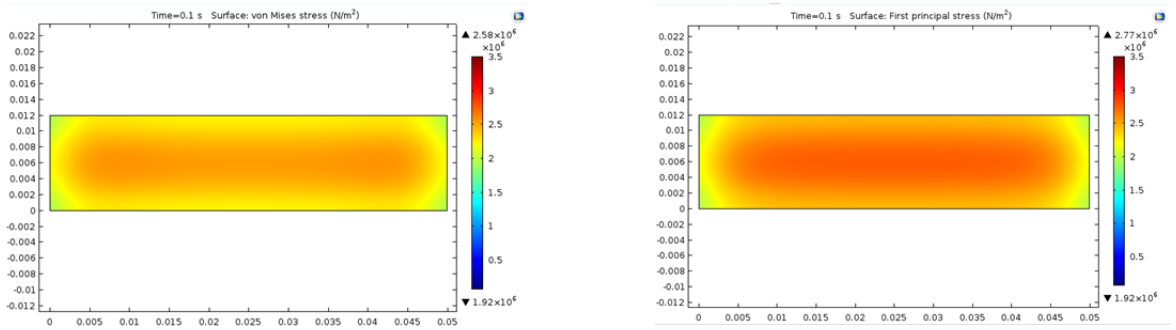

Fig. 12 Spatial distribution of first principal stress and Von Mises stress for the 12x12x50 test piece geometry – Horizontal plane located in the middle of the joint.

6x36x50mm3 joint

Changing joint configuration we observe:

- In the vertical plane, first principal stress values shows a high value near the substrate in the 4 joint corners (figure 13). However, maximum values are of the same order of magnitude as values calculated in the bulk of the material. Von Mises stress shows a more extended high stress zone along the joint perimeter nearby the substrate while the stress value in the bulk of the material is much lower.

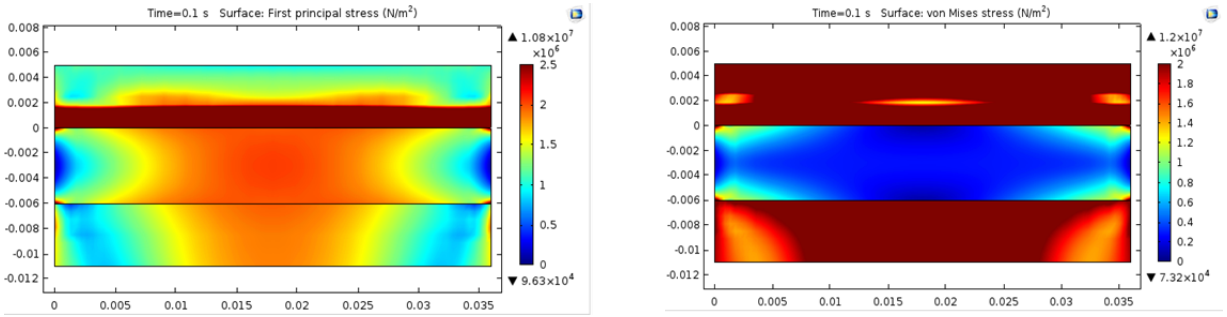

Fig. 13 Spatial distribution of first principal stress and Von Mises stress for the 6x36x50 test piece geometry – vertical plane.

- In the horizontal plane located in the middle of the joint, the first principal stress spatial distribution is inhomogeneous with a maximum value located in the center of the plane (figure 14); Maximum values are similar to maximum stress values at the interface (figure 15). Von Mises stress distribution in the middle of the joint (figure 14) is rather homogenous (except in a very thin layer along joint perimeter where stress

is low) with maximum value being five times smaller than at the interface figure 15). As a result, the ratio between the max stresses at the interface and the maximum stress in the middle of the joint is respectively 5 for Von Mises stress and 2.8 for first principal stress.

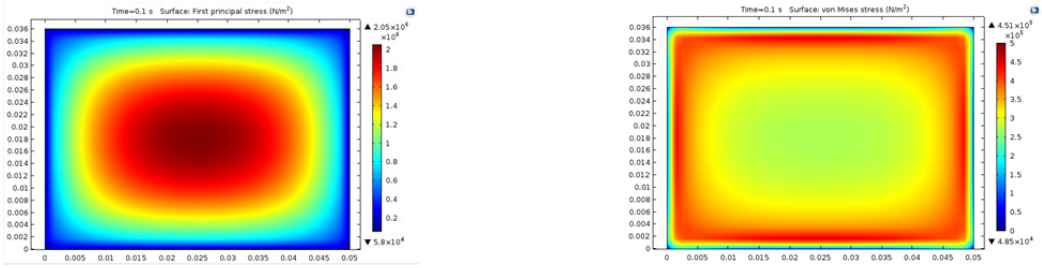

Fig. 14 Spatial distribution of first principal stress and Von Mises stress for the 6x36x50 test piece geometry – Horizontal plane located in the middle of the joint.

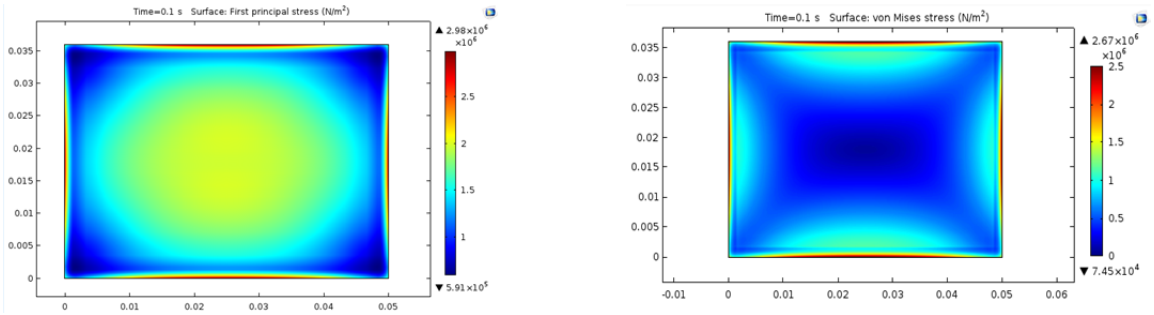

Fig. 15 Spatial distribution of first principal stress and Von Mises stress for the 6x36x50 test piece geometry – Horizontal plane located close to the substrate

Using this simplistic approach, we were not successful to predict a failure in the middle of the joint for the 12x12x50 geometry because all models show that maximum stress is located at the interface with the substrate. However, we must keep in mind that for 12x12x50 test piece, the high stress value at the interface is very local along joint perimeter.

Using Von Mises stress makes the transition in failure mode (from bulk to interfacial) when changing joint geometry more easy to understand: Von Mises stress calculated for 6x36x50 geometry shows that areas of large stress near the interface occupies a significant fraction of total gluing area while the stress distribution in the middle of the joint is very homogeneous and shows a low maximum stress value close to the average value calculated over joint cross-section.

This exercise aims to give a qualitative indication of which variable best explains location of macroscopic failure on H-pieces configurations. The next step is being able to predict when failure will take place and for a particular geometry, estimate the safety factor relative to failure. This last step is a more ambitious task. For example, we must understand if a high stress value but very local in space is critical or not: if local high stress generates a crack, this local crack may propagate and if it is case, avoiding small areas of high stress will be critical. Now, if depending on geometry, cracks propagation leads to local stress relaxation, having a very high local stress may be less damaging. Early results that shows a breakage in a middle of 12x12x50 test piece suggests that very local high stress value does not drive the failure as it would predict a failure at the interface for most of test piece configurations.

As this exercise indicated that Von Mises stresses would affect the results on sealant stress distribution within the sealant bite, we decided to compare maximum principal stresses and (maximum) Von Mises stresses for a 2D structural glazing case, varying the sealant bite. Results are shown in figure 16.

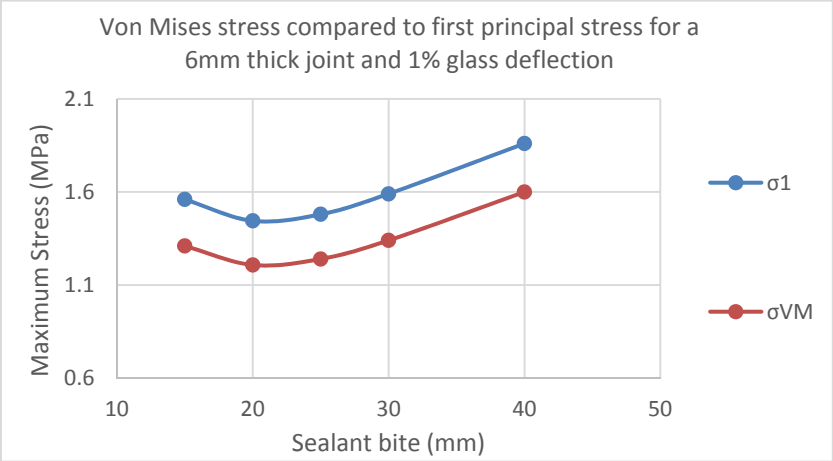

Fig. 16 Maximum Von Mises stresses compared to first principal stress in a 2D structural glazing example with 1% glass deflection.

Figure 16 confirms, for glass deflections around 1%, the existence of a saddle point in the sealant bite from which on the sealant stress increases with increasing bite, when using Von Mises stresses, in contradiction with the simplified equation generally used in structural glazing.

5. Conclusions

The study demonstrates the importance of considering glass sheet deformation in the calculation of stress built up in sealant joints of large aspect ratio. Stress distribution is very inhomogeneous and results from both the local joint rotation associated to glass pane deflection and to the shear stress induced in the joint due to the lateral displacement of the glass pane associated to deflection. Both principal stresses and Von Mises stresses show that above a 25mm bite, those local stresses increase with sealant bite and sealant stiffness (Young Modulus), a conclusion which is not in agreement with global standards for structural glazing.

The study also shows that for large glasses and high windloads, local stresses can often be reduced by applying smaller sealant bites, sealants with lower modulus or by increasing the sealant thickness, thereby decreasing the sealant aspect ratio (bite/thickness). Those conclusions are mainly valid for structural glazing sealants with high aspect ratios as the aspect ratio is generally much lower for insulating glass sealants (sealant bites: 6 to 12mm and sealant thicknesses from 12 to 20mm). Finally, a comparison was carried-out between the failure mode recorded on H-piece and the stress pattern calculated by FEA, assuming different failure theories. It appears that Von Mises stress allow to best predict the change in the type of failure mode when varying joint geometry.

References

European Technical Approval ETA-01/0005 (2006)

R. Feynman, The Feynman lectures in physics, volume II, Addison-Wesley publisher (1961-1963)

B. Kim, S. Lee, J. Lee, S. Cho, H. Park, S. Yeom & S. Park. A Comparison Among Neo-Hookean Model, Mooney-Rivlin Model, and Ogden Model for Chloroprene Rubber, International Journal of Precision Engineering and Manufacturing, May 2012, Volume 13, Issue 5, pp 759-764.